

Online Research @ Cardiff

This is an Open Access document downloaded from ORCA, Cardiff University's institutional repository: <https://orca.cardiff.ac.uk/id/eprint/104385/>

This is the author's version of a work that was submitted to / accepted for publication.

Citation for final published version:

Gualeni, B. ORCID: <https://orcid.org/0000-0002-5216-1151>, Coulman, S. A. ORCID: <https://orcid.org/0000-0002-1277-7584>, Shah, D., Eng, P.F., Ashraf, H., Vescovo, P., Blayney, G.J., Piveteau, L.-D., Guy, O.J. and Birchall, J.C. ORCID: <https://orcid.org/0000-0001-8521-6924> 2018. Minimally-invasive and targeted therapeutic cell delivery to the skin using microneedle devices. British Journal of Dermatology 178 (3) , pp. 731-739. 10.1111/bjd.15923 file

Publishers page: <http://dx.doi.org/10.1111/bjd.15923>
<<http://dx.doi.org/10.1111/bjd.15923>>

Please note:

Changes made as a result of publishing processes such as copy-editing, formatting and page numbers may not be reflected in this version. For the definitive version of this publication, please refer to the published source. You are advised to consult the publisher's version if you wish to cite this paper.

This version is being made available in accordance with publisher policies.

See

<http://orca.cf.ac.uk/policies.html> for usage policies. Copyright and moral rights for publications made available in ORCA are retained by the copyright holders.



Title: Minimally-invasive and targeted therapeutic cell delivery to the skin using microneedle devices

Running head: Microneedle cell therapy in skin

Word, table and figure count: 3529 words, 4 figures

Authors: B. Gualeni^{1,2}, S. A. Coulman^{1,2*}, D. Shah³, P. F. Eng⁴, H. Ashraf⁵, P. Vescovo⁶, G. J. Blayney⁴, L.-D. Piveteau⁶, O. J. Guy⁴, J. C. Birchall^{1,2}

Affiliations:

¹School of Pharmacy and Pharmaceutical Sciences, Redwood Building, Cardiff University, Cardiff, CF10 3NB, UK.

²Extraject Technologies Ltd, Cardiff Medicentre, Heath Park, Cardiff, CF14 4UJ, UK.

³The Hillingdon Hospital NHS Foundation Trust, Pield Heath Road, Uxbridge UB8 3NN, UK.

⁴Centre for NanoHealth, College of Engineering, Swansea University, Swansea, SA2 8PQ, UK.

⁵SPTS Technologies, Ringland Way, Newport, NP18 2TA, UK.

⁶Debiotech SA, Avenue de Sévelin 28, 1004 Lausanne, Switzerland.

*To whom correspondence should be addressed: CoulmanSA@cardiff.ac.uk

The microneedle cell delivery project is funded by Innovate UK (grant #101498) and the Welsh Government's Life Sciences Bridging Fund (grant #R3-001).

COI statement: B.G., S.A.C., D.S. and J.C.B. are inventors on the patent application WO2015132568A1 submitted by University College Cardiff Consultants Limited that covers "Microneedle based cell delivery".

Bullet statements:

- **What is already known about this topic?** Cutaneous cell therapy is currently perceived as a promising new way of treating skin damage, depigmentation and genetic disorders, and has many possible cosmetic applications.
- **What does this study add?** In this study we explore for the first time the potential of microneedle delivery systems as a novel, minimally-invasive delivery tool for facilitating cell therapy in skin.
- **What is the translational message?** A microneedle delivery platform would offer a less invasive, more controlled and targeted system for the delivery of cell therapy to skin and is thus likely to be welcomed by the patients, clinicians and regulatory bodies.

1
2
3
4
5
6
7
8
9
10
11
12
13
14
15
16
17
18
19
20
21
22
23
24
25
26
27
28
29
30
31
32
33
34
35
36
37
38
39
40
41
42
43
44
45
46
47
48
49
50
51
52
53
54
55
56
57
58
59
60

Summary: BACKGROUND: Translation of cell therapies to the clinic is accompanied by numerous challenges, including controlled and targeted delivery of the cells to their site of action, without compromising cell viability and functionality. OBJECTIVES: To explore the use of hollow microneedle devices (to date only used for the delivery of drugs and vaccines into the skin and for the extraction of biological fluids) to deliver cells into skin in a minimally-invasive, user-friendly and targeted fashion. METHODS: Melanocyte, keratinocyte and mixed epidermal cell suspensions were passed through various types of microneedles and subsequently delivered into the skin. RESULTS: Cell viability and functionality is maintained after injection through hollow microneedles with a bore size $\geq 75 \mu\text{m}$. Healthy cells are delivered into skin at clinically relevant depths. CONCLUSIONS: Hollow microneedles provide an innovative and minimally-invasive method for delivering functional cells into the skin. Microneedle cell delivery represents a potential new treatment option for cell therapy approaches including skin re-pigmentation, wound repair, scar and burn remodelling, immune therapies, and cancer vaccines.

Introduction

Cell therapies have potential application in a diverse range of disciplines¹, including dermatology. For example, autologous epidermal cell suspensions have been used clinically to treat wounds, burns, skin ulcers, scars² and skin pigmentation disorders³. Non-cutaneous cells, allogeneic cells and genetically manipulated cells have also been investigated as novel treatments for skin damage^{2,4} or to correct genetic skin disorders^{5,6} and autologous fibroblast transplantation has been approved by the Food and Drug Administration for aesthetic applications⁷. Direct accessibility to the organ makes the skin an attractive target for cell therapy approaches with approximately 90 clinical trials investigating cell therapy applications in dermatology currently active (source: <https://clinicaltrials.gov> April 2017). Translation of cell based therapies to the clinical environment is accompanied by challenges that will require innovative solutions. Controlled and targeted delivery of a cell therapy to its site of action, without compromising cell viability and functionality is one of these challenges. In this study we propose the use of microneedle devices to facilitate cell therapy applications in the skin.

Microneedles are microscopic needles that are engineered to allow for minimally-invasive perturbation of the stratum corneum barrier⁸ to deliver therapeutics both to and through skin⁹⁻¹¹ in a pain-free and blood-free fashion, with minimal skin trauma, reduced risk of infection, reduced stress in needle-phobic patients, ease of disposal, and diminished risk of needle-stick injury and cross-contamination¹². Microneedles have been microfabricated in a range of materials⁹, geometries and spatial arrangements¹⁰. The shape, length, width and sharpness of microneedles can be adapted¹¹ and, depending on the application, microneedles can be arranged as a single-needle, a row of needles or an array of protrusions for insertion into skin by hand, or with the assistance of an applicator device¹³. Many studies have shown the utility of

microneedle devices for the intradermal delivery of low molecular weight drugs, biological therapies and vaccines^{10,13,14}. Microneedle systems have also been used to extract blood and interstitial fluid for real-time monitoring of biomarkers^{15,16}. This study is the first to exploit microneedles for the targeted delivery of cells into skin and aims to exemplify the potential of microneedle-mediated cell delivery for the minimally-invasive treatment of vitiligo.

Vitiligo is a skin condition, with a prevalence of approximately 1% worldwide^{17,18}, characterised by the development of de-pigmented patches on the skin, hair or both, caused by the localised death or loss of function of the pigment-producing melanocytes. The current theory is that vitiligo is caused by altered inflammatory and immune responses¹⁹⁻²², with genetic and environmental factors²³⁻²⁸ also playing important roles. There is no definitive cure for vitiligo, with current treatments aiming to maintain and restore pigmentation. As a first line of treatment, patients are offered topical treatments such as corticosteroids or calcineurin inhibitors, followed by a combination of UV-light therapy and systemic steroid treatment, however treatment failure using these approaches is common³¹. Surgical treatments (i.e. tissue grafts or cellular grafts) can be considered in patients with segmental vitiligo or with non-segmental vitiligo that has been stable for at least 12 months after documented non-responsive medical treatment. These surgical approaches have comparable re-pigmentation success rate, but cellular grafts permit treatment of larger areas of skin and have better cosmetic results³². The two currently available commercial kits for cellular grafting, ReCell[®] (Avita Medical) and Viticell[®] (Laboratoires Genévrier), whilst effective, rely upon laser abrasion or dermabrasion to prepare the recipient skin site³³. These are invasive, time consuming techniques, that require the use of local anaesthetics and carry the risk of scarring, skin discolouration, infections and bleeding³⁴. Once the outer skin layers have been removed by abrasion methods, healthy, non-cultured cells taken from a patients' own skin (i.e.

1
2
3 autologous cells) are applied to the exposed skin in the form of a topical cell suspension or an
4 aerosolised spray. The treated area is then dressed to enhance cell survival and attachment,
5
6 protect from trauma and reduce infection risk³⁵.
7
8
9

10 In this study we investigate the use of hollow microneedles for the minimally-invasive delivery
11 of autologous cells to human skin and aim to exemplify their potential for cellular grafting in
12 vitiligo. A microneedle delivery system for cellular grafting would negate the need for skin
13 abrasion (to prepare the recipient site) and dressing (after the procedure), thus reducing
14 procedural pain, post-procedural discomfort and the risk of infection for vitiligo patients. It
15 would also dramatically reduce the need for immobilisation after treatment, making it suitable
16 for anatomical sites that are currently perceived as difficult to treat (e.g. lips and finger joints).
17 Microneedles therefore offer a less invasive, more controlled and targeted means of cell delivery
18 that is likely to reduce cell loss, enhance efficacy and thus gain greater acceptance by the
19 patients, clinicians and regulatory bodies.
20
21
22
23
24
25
26
27
28
29
30
31
32
33
34
35
36

37 **Materials and Methods**

38 *Microneedles*

39
40 A range of hollow silicon microneedles were manufactured by photolithography and deep silicon
41 etching at Swansea University and SPTS Technologies. Rows of 5 or 6 microneedles and 3-
42 dimensional arrays of 5×5 microneedles with bore sizes ranging from 75 to 150 µm were
43 fabricated to investigate the effect of needle bore size on cell delivery.
44
45
46
47
48
49
50

51 Single hollow silicon microneedles (DebioJect™) of 80 µm bore size and lengths of 400, 500,
52 600 or 700 µm, with apertures 200 µm from the tip, were supplied by Debiotech S. A.,
53 Switzerland to investigate the effect of needle length on the depth of cell delivery to skin.
54
55
56
57
58
59
60

Human skin tissue

Freshly excised human breast skin was obtained from surgical procedures under full ethical approval and informed patient consent (LREC Ref: 08/WSE03/55).

Human epidermal cell suspensions

Epidermal cell suspensions (ECS) were prepared using a method adapted from previously reported work^{3,36}. Cells were re-suspended in PBS, counted, diluted to a concentration of 1.5×10^6 cell/mL and either seeded in culture dishes with cell selective media or used for cell survival and skin delivery experiments.

Melanocyte and keratinocyte cell cultures

Commercial primary melanocytes and keratinocytes (Life Technologies) were seeded at a density of 5×10^3 cell/cm² in medium 254 (Life Technologies) or 2.5×10^3 cell/cm² in EpiLife medium (Life Technologies) respectively. The media were supplemented with 1% PMA-free human melanocyte or keratinocyte growth supplement (Life Technologies) respectively, and 1% Penicillin/Streptomycin/Amphotericin B solution (Merck Millipore).

To select melanocytes or keratinocytes from the skin-derived ECS, cells were seeded at a density of 5×10^4 cell/cm² in the appropriate selective growth media, as detailed previously. After two passages in selective media, pure melanocyte or keratinocyte cell cultures were obtained.

Cell viability and functionality

Cell viability and functionality tests were performed with ECS, cultured melanocytes and cultured keratinocytes, each at concentrations of 10^5 , 10^6 and 10^7 cells/mL. Aliquots of cell suspension mixed with an equal volume of trypan blue solution 0.4% (Life Technologies) were tested before (baseline) and after passing through a syringe, either without (control) or with hollow microneedles attached. Stained (non-viable) and unstained (viable) cells were counted under a light microscope (IX50, Olympus) using a haemocytometer to calculate cell survival rates.

To determine cell functionality, the extruded cells were seeded and cultured in appropriate cell media. Cell adhesion was evaluated after 24 hours and cell proliferation was assessed every 48 hours. Cell phenotype was visually examined using the IX50 light microscope. Phenotype was also biochemically assessed by western blot on cell lysates 72 hours after confluence, or by immunofluorescence using either a fluorescence microscope (DM IRB, Leica Microsystems) or a confocal microscope (TCS SP5, Leica Microsystems).

Western Blot

72 hours after confluence, cells were lysed with 1 mL of RIPA lysis and extraction buffer (VWR). Cell lysates were loaded on an SDS-Page 10% precast gel (Bio-Rad Laboratories) and run at 120 V for 70 minutes. Electrophoretic transfer on a nitrocellulose membrane was performed using a Trans Blot Turbo Transfer System (Bio-Rad Laboratories) at 25V for 30 minutes. The mouse monoclonal anti melan-A antibody (clone M2-7C10, Abcam) was used to confirm the melanocytic phenotype at a dilution of 1:500. The mouse monoclonal anti beta-actin antibody (Abcam) was used as a loading control at a dilution of 1:1000.

Immunofluorescence of cells

Cultured cells were grown on glass coverslips for 72 hours, fixed in cold acetone (Fisher Scientific), washed in PBS, incubated with 0.1% Triton X-100 (Sigma) for 15 minutes, washed in PBS, and blocked with 10% goat serum (Sigma) for 30 minutes. Cells were incubated with primary antibody overnight at 4°C. The mouse monoclonal anti melan-A antibody (1:200) and the rabbit polyclonal anti involucrin antibody (Abcam, 1:200) were used to confirm the melanocytic and the keratinocytic phenotypes respectively. Cells were then washed and incubated with secondary antibodies goat anti mouse IgG H&L AlexaFluor® 448 and goat anti rabbit IgG H&L AlexaFluor® 647 (Abcam, 1:1000) for 1 hour. Nuclei were stained with 10 µm Hoechst 33342 (Life Technologies) for 10 minutes. Coverslips were mounted cell-face down onto Superfrost™ Plus slides (VWR) and imaged using a Retiga EXi digita camera (QImaging) connected to the DM IRB fluorescence microscope or the TCS SP5 confocal microscope.

Depth of microneedle penetration in ex vivo human skin

Following microneedle insertion into *ex vivo* human skin, disruption in the tissue was visualised using either a non-invasive VivoSight optical coherence tomography (OCT) clinical imaging system (Michelson Diagnostics) or classic histology on 10 µm thick transverse cryosections of the microneedle treated area of skin.

Skin healing kinetics in vivo

Skin healing was assessed *in vivo* following insertion of the DebioJect™ microneedles using a high velocity applicator. Human volunteers (N=5) aged between 18 and 30 years were recruited under informed consent with local ethics committee approval. The microneedle insertion site was

1
2
3 imaged using the VivoSight OCT clinical imaging system before microneedle insertion,
4
5 immediately after, and then at 30 minutes, 1 hour, 2 hours, 4 hours and 24 hours post-insertion to
6
7 evaluate the kinetics of microchannel closure.
8
9

10 11 12 *Cell distribution in ex vivo human skin*

13
14 Cell nuclei were stained with 10 μ M Hoechst 33342 and cells were re-suspended in PBS at
15
16 concentrations of either 10^6 or 10^7 cells/mL. 50 μ L of these suspensions were injected into *ex*
17
18 *vivo* human skin using microneedles. The injected area was excised within 5 minutes of injection
19
20 using 6 mm biopsy punches (Miltex) and processed for cryosectioning. 10 μ m thick transverse
21
22 cryosections were mounted on Superfrost™ Plus slides and observed under the DM IRB
23
24 fluorescence microscope to evaluate cell distribution in skin following delivery via microneedles.
25
26
27
28
29
30

31 32 *Immunofluorescence in skin*

33
34 For immunofluorescence experiments in skin, 10 μ m thick cryosections were incubated in
35
36 primary antibody solution (1:200 rabbit polyclonal anti involucrin antibody and 1:200 mouse
37
38 monoclonal anti melan-A antibody) overnight at 4°C. Sections were then washed in PBS and
39
40 incubated in secondary antibody solution (1:1000 goat anti mouse IgG H&L AlexaFluor® 448
41
42 and 1:1000 goat anti rabbit IgG H&L AlexaFluor® 647) for 1 hour. Slides were mounted and
43
44 imaged to confirm cell phenotype after delivery to skin via microneedles.
45
46
47
48
49

50 51 *Statistical analysis*

52
53 Where applicable, statistical differences were evaluated using Student's *t*-test and results were
54
55 expressed as means \pm S.E.M. A value of $p < 0.05$ was considered statistically significant.
56
57
58
59
60

Results

Cell numbers and viability are maintained following extrusion through microneedles.

Cultured melanocytes, cultured keratinocytes, and non cultured epidermal cell suspensions (NCECS) at concentrations ranging from 10^5 to 10^7 cells/mL were passed through microneedles. Our preliminary data indicated that cell survival was strongly reduced when cells were extruded through apertures with a diameter less than $75\text{ }\mu\text{m}$, therefore our studies focused on microneedles with a bore size $\geq 75\text{ }\mu\text{m}$. Cell counts before (baseline) and after extrusion through a syringe, both without (control) or with microneedles attached via a Luer fit adaptor, revealed that cell numbers were maintained during the injection process (Fig. 1 A and B; Supplemental Table 1).

Furthermore, studies using a trypan blue exclusion method confirmed that cell survival was not adversely affected after passage through microneedles with a bore size $\geq 75\text{ }\mu\text{m}$ (Fig. 1 C and D; Supplemental Table 2).

Cell functionality is maintained following extrusion through microneedles.

Following extrusion through microneedles and overnight incubation in appropriate culture media, all cell types displayed normal adhesion to the culture dishes. After 48 hours of incubation cells had assumed their distinctive morphologies, according to their phenotypes (Fig. 2A). Cell phenotype was also confirmed biochemically by western blot (Fig. 2B) and immunofluorescence (Fig. 2C). All cell types tested maintained their phenotype after extrusion through microneedles with a bore size $\geq 75\text{ }\mu\text{m}$.

Hollow microneedles penetrate ex vivo and in vivo skin efficiently.

1
2
3 The ability of the microneedles to effectively and reliably puncture human skin *ex vivo* and *in*
4 *vivo* was assessed. Methylene blue staining confirmed that microneedles penetrate *ex vivo* skin
5 reliably when inserting either a row of microneedles manually (Fig. 3A) or a single microneedle
6 using an applicator (Fig. 3B). Efficient microneedle skin penetration *ex vivo* was also confirmed
7 by histology (Fig. 3C) and optical coherence tomography (OCT) imaging (Fig. 3D). The depth of
8 tissue disruption was between 60 and 250 μm , irrespective of the length of the microneedle used.
9 Data obtained from OCT imaging in human volunteers (N=5) at different time points following
10 insertion and removal of DebioJect™ indicates that complete closure of the microchannels
11 created by the microneedle takes between 4 and 24 hours *in vivo* (Fig. 3E).
12
13
14
15
16
17
18
19
20
21
22
23
24
25
26

27 *Microneedles can efficiently deliver cells to ex vivo human skin.*

28
29 Pre-labelled cell suspensions were injected into skin (50 μL at 10^6 or 10^7 cells/mL concentration)
30 using single microneedles of 80 μm bore size and different lengths (between 400 and 700 μm) or
31 rows of microneedles of 100 μm bore size and length of 600 μm (N=4 per condition). Cell
32 distribution in the skin was tracked using fluorescence microscopy. Regardless of microneedle
33 length, cells were deposited in the upper dermis, generally towards the boundary of the reticular
34 and papillary dermis (Fig. 4).
35
36
37
38
39
40
41
42

43 Injections performed using a single microneedle resulted in cells being deposited proximal to the
44 microneedle insertion point (Fig. 4A, top row). Injections using rows of microneedles resulted in
45 multiple points of dermal deposition associated with the loci of microneedle penetration (Fig.
46 4A, middle row). Shorter microneedles (400 μm) were able to deliver cells slightly more
47 superficially (towards the epidermal-dermal junction), however needle insertion and liquid
48 injection was less reliable (Fig. 4A, bottom row).
49
50
51
52
53
54
55
56
57
58
59
60

Cells maintain their functionality when injected into skin

Frozen sections of *ex vivo* human skin that had been injected with labelled NCECS via microneedles were used to assess cell functionality following skin delivery. Some of the injected cells (Fig. 4B, labelled blue nuclei) clearly express markers of melanocytic (green cytoplasm) or keratinocytic (red cytoplasm) differentiation, indicating that cells maintain their phenotype following skin delivery.

Discussion

Microneedles of different materials, shapes, lengths, and spatial arrangements have been exploited pre-clinically and clinically for drug delivery, vaccination and biosensing applications. In this study we explored the use of hollow microneedles for delivering cells to skin, thus providing a minimally-invasive technology platform for the delivery of cell therapies. Cell delivery via microneedles was examined using silicon devices with bore sizes $\geq 75 \mu\text{m}$. A range of individual and mixed cell types (i.e. human melanocytes, human keratinocytes and mixtures of epidermal cells derived from fresh human skin explants) and three clinically relevant cell concentrations (10^5 , 10^6 or 10^7 cells/mL) were specifically selected to demonstrate broad clinical applicability of the microneedle cell delivery system. Effective extrusion of cell suspensions through the microneedles, with no loss of cells at all of the tested conditions, indicates that neither cell adhesion to the inner surfaces of the device, aggregation of the biological material or physical obstruction of the microneedle aperture impede effective delivery of the cells. The viability of cells was preserved following microneedle injection. The only statistically significant ($p < 0.05$) reduction in cell survival was observed when extruding NCECS at the concentration of

1
2
3 10⁶ cells/mL through microneedles with a bore size of 150 µm ($p=0.04$). However, cell survival
4
5 at this concentration was not affected when passing through smaller aperture microneedles,
6
7 suggesting that this may be an anomalous result. Our data indicates that the integrity of the cell
8
9 membrane is maintained when cells are extruded through apertures of 75-150 µm, however a 150
10
11 µm aperture should not be considered an upper limit; increasing the dimensions of the
12
13 microchannels is likely to further reduce the sheer forces exerted on cells, facilitating their
14
15 survival.
16
17
18

19
20 All cell types investigated maintained their distinctive phenotype after extrusion through
21
22 microneedles and at all concentrations tested. This was evidenced by retention of typical
23
24 morphological features and expression of specific intracellular markers. From a clinical
25
26 perspective, it is encouraging that microneedle injection of a range of cell types and
27
28 concentrations is possible and the injection process does not adversely affect cell viability and
29
30 functionality.
31
32
33

34 Success of the microneedle device as a platform for cutaneous cell therapy applications,
35
36 including vitiligo and wound healing, is initially dependent on reliable insertion of the needle
37
38 into the tissue. The microneedles used in this study punctured both *ex vivo* (human skin explant)
39
40 and *in vivo* (human volunteer) skin reproducibly. The observable depth of the microchannels that
41
42 remained in the skin following the removal of the microneedles was measured in skin explants
43
44 and was found to be between 60 and 250 µm, regardless of the length and the type of
45
46 microneedles used. The small dimensions of these microchannels is likely to be the result of
47
48 sealing of the puncture site, in which the elasticity of the dermal tissue enables physical closure
49
50 of the perturbation. OCT data exploring the *in vivo* kinetics of skin closure in young adults
51
52 confirms the physical dimensions of the skin disruption immediately following microneedle
53
54
55
56
57
58
59
60

1
2
3
4
5
6
7
8
9
10
11
12
13
14
15
16
17
18
19
20
21
22
23
24
25
26
27
28
29
30
31
32
33
34
35
36
37
38
39
40
41
42
43
44
45
46
47
48
49
50
51
52
53
54
55
56
57
58
59
60

insertion and removal. Monitoring the same skin puncture site over time in human subjects demonstrates the organ’s wound healing capabilities to ensure restoration of the biological barrier. These studies suggest that healing of the more superficial cellular epidermis layer begins relatively quickly, with restoration of the visible skin barrier 4 - 24 hours after microneedle application.

Having established cell survival and functionality following extrusion through microneedles that are able to penetrate human skin, an excised human skin model³⁷ was used to investigate intradermal cell delivery. These studies used microneedles with different spatial arrangements (single and rows) and lengths (from 400 µm to 700 µm), and clinically relevant volumes and concentrations of cell suspensions. Regardless of the length of the devices, hollow microneedles deposited cells in the upper dermis. The shortest microneedles available (400 µm) facilitated more superficial delivery, predominantly in the papillary dermis, but delivery efficiency was less reproducible due to incomplete insertion of the microneedle below the depth of the bore and resulting leakage of the cell suspension onto the skin surface. This suggests that hollow microneedles at least 500 µm in length may be more appropriate for cell delivery to the skin, with longer microneedles used for applications that require deposition in the deep dermis. After deposition, cells did not distribute widely from the injection site, tending to cluster in an area proximal to the point of microneedle insertion. Therefore, multiple microneedles can be employed for therapeutic applications that require cell delivery over a wider surface area (e.g. for the treatment of extensive vitiliginous patches on the arms and legs), while the use of single microneedles could be more appropriate when more precise delivery is needed (e.g. for the treatment of small de-pigmented areas around the eyes, lips or finger joints of vitiligo patients).

1
2
3 This study aimed to exemplify the potential of microneedle-assisted cell delivery in the context
4
5 of vitiligo treatment. Current cell therapy procedures in vitiligo patients require dermabrading
6
7 the skin, a procedure that is painful and prone to scarring, and then applying a topical cell
8
9 therapy. Delivering an autologous, non-cultured cell suspension to a de-pigmented site using
10
11 microneedles will be less painful for patients, with a reduced risk of scarring and infection. This
12
13 will also reduce the inefficiency (i.e. cell loss) associated with topical application and will negate
14
15 the need to immobilise the patient after treatment, representing a significant clinical advantage.
16
17
18 Cell therapy for vitiligo aims to restore a functional melanocyte population to the basal
19
20 epidermis, however all hollow microneedles tested in this study deposited the NCECS in the
21
22 upper dermis. Published research indicates that following an intradermal injection of NCECS
23
24 using a 30G hypodermic needle, melanocytes are able to migrate to the basal layer, where they
25
26 start producing melanin, inducing re-pigmentation³⁸. Therefore, following microneedle delivery,
27
28 melanocytes will be expected to migrate to the basal layer of the viable epidermis in response to
29
30 local signalling, and produce melanin to re-pigment the skin. The use of multiple microneedles to
31
32 deliver multiple pockets of cells would negate the need for lateral diffusion of melanocytes. We
33
34 are now conducting a first-in-human pilot study to test the safety and efficacy of microneedles
35
36 for cell delivery in vitiligo patients.
37
38
39
40
41
42

43 In conclusion, we have shown for the first time that hollow microneedles are an appropriate
44
45 delivery technology for precise, minimally-invasive cell therapy applications in the skin.
46
47 Microneedles of appropriate length, bore size and spatial arrangement can deliver cells to
48
49 appropriate compartments of the skin across a clinically relevant surface area. Cell therapy is a
50
51 new and exciting clinical application for these versatile medical devices, with microneedles
52
53 being readily adaptable for simple and targeted delivery of various cells (including, but not
54
55
56
57
58
59
60

1
2
3
4
5
6
7
8
9
10
11
12
13
14
15
16
17
18
19
20
21
22
23
24
25
26
27
28
29
30
31
32
33
34
35
36
37
38
39
40
41
42
43
44
45
46
47
48
49
50
51
52
53
54
55
56
57
58
59
60

restricted to, keratinocytes, Langerhans cells, dendritic cells, stem cells, T cells, fibroblasts, melanocytes, Merkel cells, mast cells and macrophages) into skin compartments for a variety of therapeutic and cosmetic applications, including treatment of vitiligo and post-inflammatory depigmentation, scar and burn remodelling and re-pigmentation, wound and skin ulcer repair, immune therapies, and cancer vaccines.

REFERENCES

- 1 Trounson A, DeWitt ND. Pluripotent stem cells progressing to the clinic. *Nat Rev Mol Cell Biol* 2016; **17**: 194 200.
- 2 You HJ, Han SK. Cell therapy for wound healing. *J Korean Med Sci* 2014; **29**: 311 9.
- 3 Gauthier Y, Benzekri L. Non cultured epidermal suspension in vitiligo: from laboratory to clinic. *Indian J Dermatol Venereol Leprol* 2012; **78**: 59 63.
- 4 Zhang C, Chen Y, Fu X. Sweat gland regeneration after burn injury: is stem cell therapy a new hope? *Cytotherapy* 2015; **17**: 526 35.
- 5 Wenzel D, Bayerl J, Nyström A *et al*. Genetically corrected iPSCs as cell therapy for recessive dystrophic epidermolysis bullosa. *Sci Transl Med* 2014; **6**: 264ra165.
- 6 Wagner JE, Ishida Yamamoto A, McGrath JA *et al*. Bone marrow transplantation for recessive dystrophic epidermolysis bullosa. *N Engl J Med* 2010; **363**: 629 39.
- 7 Weiss RA. Autologous cell therapy: will it replace dermal fillers? *Facial Plast Surg Clin North Am* 2013; **21**: 299 304.
- 8 Henry S, McAllister DV, Allen MG *et al*. Microfabricated microneedles: a novel approach to transdermal drug delivery. *J Pharm Sci* 1998; **87**: 922 5.
- 9 Tuan Mahmood TM, McCrudden MT, Torrisi BM *et al*. Microneedles for intradermal and transdermal drug delivery. *Eur J Pharm Sci* 2013; **50**: 623 37.
- 10 McAllister DV, Allen MG, Prausnitz MR. Microfabricated microneedles for gene and drug delivery. *Annu Rev Biomed Eng* 2000; **2**: 289 313.
- 11 van der Maaden K, Jiskoot W, Bouwstra J. Microneedle technologies for (trans)dermal drug and vaccine delivery. *J Control Release* 2012; **161**: 645 55.
- 12 Birchall JC, Clemo R, Anstey A *et al*. Microneedles in clinical practice -an exploratory study into the opinions of healthcare professionals and the public. *Pharmaceutical research* 2011; **28**: 95 106
- 13 Prausnitz MR. Microneedles for transdermal drug delivery. *Adv Drug Deliv Rev* 2004; **56**: 581 7
- 14 Kim YC, Park JH, Prausnitz MR. Microneedles for drug and vaccine delivery. *Adv Drug Deliv Rev* 2012; **64**: 1547 68
- 15 Donnelly RF, Mooney K, Caffarel Salvador E *et al*. Microneedle mediated minimally invasive patient monitoring. *Therapeutic drug monitoring* 2014; **36**: 10 7
- 16 Wang PM, Cornwell M, Prausnitz MR. Minimally invasive extraction of dermal interstitial fluid for glucose monitoring using microneedles. *Diabetes technology & therapeutics* 2005; **7**: 131 41.
- 17 Ezzedine K, Eleftheriadou V, Whitton M *et al*. Vitiligo. *Lancet* 2015; **386**: 74 84.
- 18 Krüger C, Schallreuter KU. A review of the worldwide prevalence of vitiligo in children/adolescents and adults. *Int J Dermatol* 2012; **51**: 1206 12.
- 19 Rezaei N, Gavalas NG, Weetman AP *et al*. Autoimmunity as an aetiological factor in vitiligo. *J Eur Acad Dermatol Venereol* 2007; **21**: 865 76
- 20 Mosenson JA, Eby JM, Hernandez C *et al*. A central role for inducible heat shock protein 70 in autoimmune vitiligo. *Exp Dermatol* 2013; **22**: 566 9.
- 21 Boniface K, Taïeb A, Seneschal J. New insights into immune mechanisms of vitiligo. *G Ital Dermatol Venereol* 2016; **151**: 44 54.
- 22 Strassner JP, Harris JE. Understanding mechanisms of autoimmunity through translational research in vitiligo. *Curr Opin Immunol* 2016; **43**: 81 8
- 23 Spritz RA. The genetics of generalized vitiligo: autoimmune pathways and an inverse relationship with malignant melanoma. *Genome Med* 2010; **2**: 78.
- 24 Jin Y, Birlea SA, Fain PR *et al*. Genome wide association analyses identify 13 new susceptibility loci for generalized vitiligo. *Nat Genet* 2012; **44**: 676 80
- 25 van den Boorn JG, Picavet DI, van Swieten PF *et al*. Skin depigmenting agent monobenzone induces potent T cell autoimmunity toward pigmented cells by tyrosinase haptentation and melanosome autophagy. *J Invest Dermatol* 2011; **131**: 1240 51.
- 26 Jeon IK, Park CJ, Lee MH *et al*. A Multicenter Collaborative Study by the Korean Society of Vitiligo about Patients' Occupations and the Provoking Factors of Vitiligo. *Ann Dermatol* 2014; **26**: 349 56.
- 27 Vrijman C, Hosseinpour D, Bakker JG *et al*. Provoking factors, including chemicals, in Dutch patients with vitiligo. *Br J Dermatol* 2013; **168**: 1003 11

28 Hariharan V, Klarquist J, Reust MJ *et al.* Monobenzyl ether of hydroquinone and 4-tertiary butyl phenol activate markedly different physiological responses in melanocytes: relevance to skin depigmentation. *J Invest Dermatol* 2010; **130**: 211-20.

29 Jimbow K, Chen H, Park JS *et al.* Increased sensitivity of melanocytes to oxidative stress and abnormal expression of tyrosinase-related protein in vitiligo. *Br J Dermatol* 2001; **144**: 55-65.

30 Xie H, Zhou F, Liu L *et al.* Vitiligo: How do oxidative stress-induced autoantigens trigger autoimmunity? *J Dermatol Sci* 2016; **81**: 3-9.

31 Speeckaert R, Speeckaert MM, van Geel N. Why treatments do(n't) work in vitiligo: An autoinflammatory perspective. *Autoimmun Rev* 2015; **14**: 332-40.

32 Taieb A, Alomar A, Böhm M *et al.* Guidelines for the management of vitiligo: the European Dermatology Forum consensus. *Br J Dermatol* 2013; **168**: 5-19.

33 Mulekar SV, Ghwish B, Al Issa A *et al.* Treatment of vitiligo lesions by ReCell vs. conventional melanocyte-keratinocyte transplantation: a pilot study. *Br J Dermatol* 2008; **158**: 45-9.

34 Friedman S, Lippitz J. Chemical peels, dermabrasion, and laser therapy. *Dis Mon* 2009; **55**: 223-35.

35 Al-Hadidi N, Griffith JL, Al-Jamal MS *et al.* Role of Recipient-site Preparation Techniques and Post-operative Wound Dressing in the Surgical Management of Vitiligo. *J Cutan Aesthet Surg* 2015; **8**: 79-87.

36 Migliano E, Bellei B, Govoni FA *et al.* Fat and epidermal cell suspension grafting: a new advanced one-step skin regeneration surgical technique. *J Exp Clin Cancer Res* 2014; **33**: 23.

37 Groves RB, Coulman SA, Birchall JC *et al.* An anisotropic, hyperelastic model for skin: experimental measurements, finite element modelling and identification of parameters for human and murine skin. *J Mech Behav Biomed Mater* 2013; **18**: 167-80.

38 Khodadadi L, Shafieyan S, Sotoudeh M *et al.* Intraepidermal injection of dissociated epidermal cell suspension improves vitiligo. *Arch Dermatol Res* 2010; **302**: 593-9.

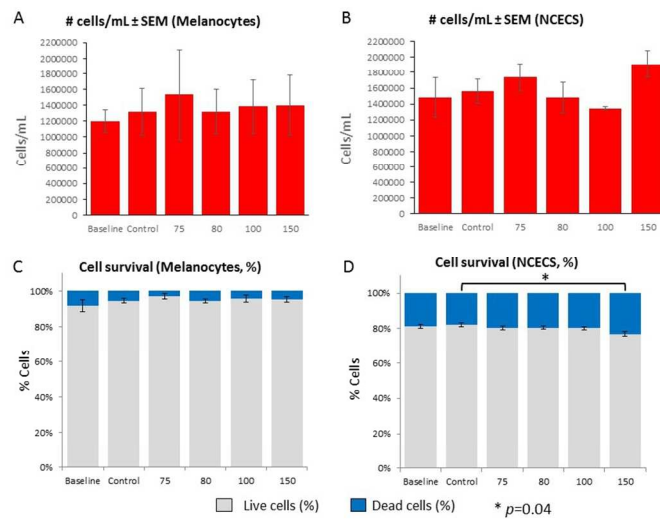
Figure legends

Figure 1. Cell numbers and cell viability are maintained after extrusion through microneedles. Melanocytes (A, C) or non-cultured epidermal cell suspensions (NCECS, B, D) were counted before (in this case 10^6 cells/mL) and after extrusion through microneedles (A, B). No significant cell loss was observed. Results are expressed as number of cells/mL \pm SEM (N=3). Viability studies (C, D) using a trypan blue exclusion method indicate there are no significant changes after extrusion of a cell solution of 10^6 cells/mL, apart from a reduction in cell survival when NCECS were extruded through 150 μ m bore size microneedles compared to control samples (* $p=0.04$). Results are expressed in % cells \pm SEM (N=3).

Figure 2. Cell functionality is maintained after extrusion through microneedles. (A) After 48 hours of incubation, cells extruded through microneedles with 75, 80, 100 and 150 μ m bore size had assumed their distinctive morphologies. Scale bars = 100 μ m. (B) Cell lysates obtained from melanocytes cultured for 72 h after being passed through microneedles of different bore sizes show that cells still express the melanocytic marker melan-A. +ve=positive control (melanocyte culture), -ve=negative control (keratinocyte culture), β -actin=loading control. (C) Confocal microscopy images of an ECS grown on glass coverslips for 72 hours after extrusion through microneedles of different bore sizes show that melanocytes (positive to melan-A, green) and keratinocytes (positive to involucrin, red) have maintained their phenotypes. Scale bars = 50 μ m.

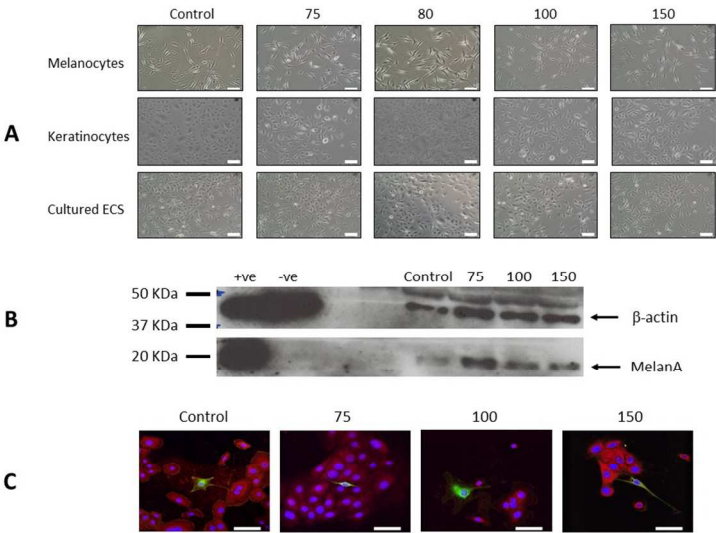
Figure 3. Microneedle penetration of human skin. Methylene blue staining of *ex vivo* human skin reveals efficient skin penetration following manual insertion (**A**) and applicator-assisted insertion (**B**) of microneedles. Classic histology (**C**) and Optical Coherence Tomography (OCT) (**D**) also confirm efficient skin penetration (blue arrows highlight the microchannels remaining in the skin after microneedle application). Scale bars = 200 μm . SC: Stratum corneum; Ep: Epidermis; De: Dermis. Skin healing *in vivo* (**E**) was measured using OCT up to 24 hours after microneedle (700 μm) insertion into human volunteers (N=5).

Figure 4. Microneedle-mediated cell delivery to human skin. (**A**) Fluorescence microscopy of cryosections from human skin explants injected with labelled NCECS (blue) at a concentration of 10^7 cells/mL reveals that the cells are mainly delivered to the upper dermis. The images shown are from injections performed with a single microneedle of 700 μm length (Single), a row of microneedles of 600 μm length (Row), or a single microneedle of 400 μm length (Short). The red dashed line indicates the epidermal/dermal junction (epidermis above and dermis below the line). The red asterisk indicates the insertion point, the yellow asterisks mark the clusters of injected cells, and the yellow arrows point at the cells injected in the basal layer. (**B**) Confocal microscopy images of cryosections of excised human skin injected with labelled ECS and incubated with anti melan-A and anti involucrin antibodies show that the injected cells (blue nuclei) maintain their melanocytic (green cytoplasm, green arrow) or keratinocytic (red cytoplasm, red arrow) phenotype after delivery. Scale bars = 100 μm .



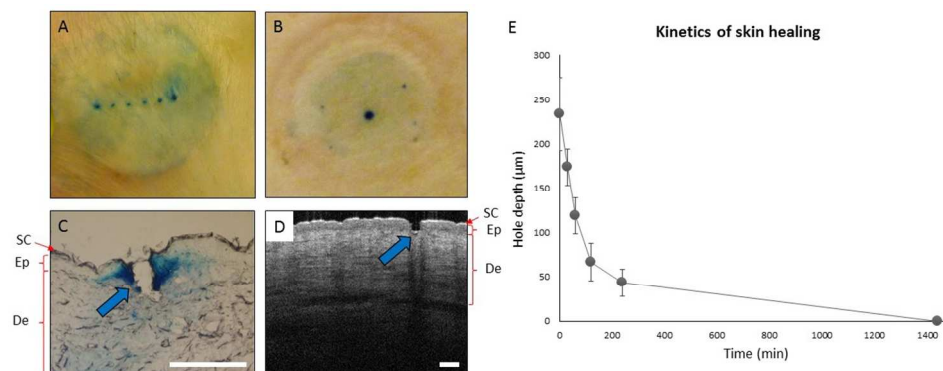
Cell numbers and cell viability are maintained after extrusion through microneedles. Melanocytes (A, C) or non-cultured epidermal cell suspensions (NCECS, B, D) were counted before (in this case 106 cells/mL) and after extrusion through microneedles (A, B). No significant cell loss was observed. Results are expressed as number of cells/mL \pm SEM (N=3). Viability studies (C, D) using a trypan blue exclusion method indicate there are no significant changes after extrusion of a cell solution of 106 cells/mL, apart from a reduction in cell survival when NCECS were extruded through 150 μ m bore size microneedles compared to control samples (* $p=0.04$). Results are expressed in % cells \pm SEM (N=3).

338x190mm (96 x 96 DPI)



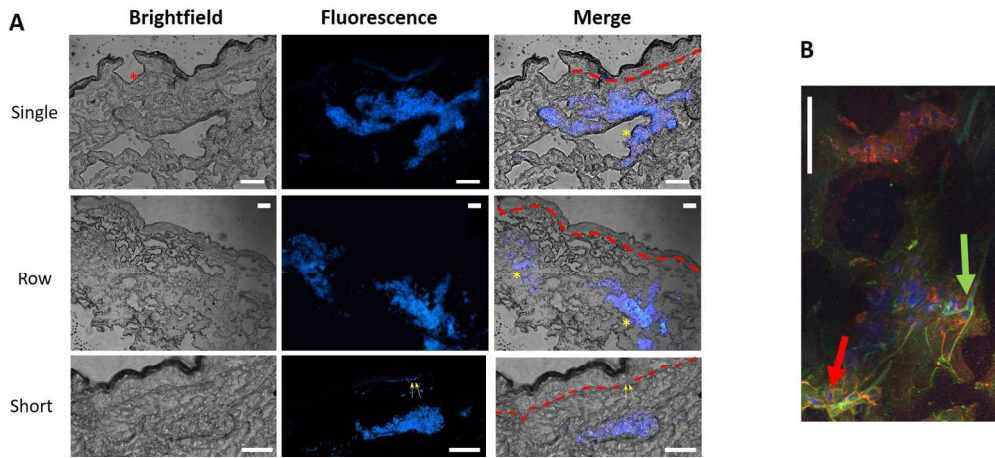
Cell functionality is maintained after extrusion through microneedles. (A) After 48 hours of incubation, cells extruded through microneedles with 75, 80, 100 and 150 μm bore size had assumed their distinctive morphologies. Scale bars = 100 μm . (B) Cell lysates obtained from melanocytes cultured for 72 h after being passed through microneedles of different bore sizes show that cells still express the melanocytic marker melan-A. +ve=positive control (melanocyte culture), -ve=negative control (keratinocyte culture), β -actin=loading control. (C) Confocal microscopy images of an ECS grown on glass coverslips for 72 hours after extrusion through microneedles of different bore sizes show that melanocytes (positive to melan-A, green) and keratinocytes (positive to involucrin, red) have maintained their phenotypes. Scale bars = 50 μm .

338x190mm (96 x 96 DPI)



Microneedle penetration of human skin. Methylene blue staining of ex vivo human skin reveals efficient skin penetration following manual insertion (A) and applicator-assisted insertion (B) of microneedles. Classic histology (C) and Optical Coherence Tomography (OCT) (D) also confirm efficient skin penetration (blue arrows highlight the microchannels remaining in the skin after microneedle application). Scale bars = 200 μm . SC: Stratum corneum; Ep: Epidermis; De: Dermis. Skin healing in vivo (E) was measured using OCT up to 24 hours after microneedle (700 μm) insertion into human volunteers (N=5).

338x190mm (96 x 96 DPI)



Microneedle-mediated cell delivery to human skin. (A) Fluorescence microscopy of cryosections from human skin explants injected with labelled NCECS (blue) at a concentration of 107 cells/mL reveals that the cells are mainly delivered to the upper dermis. The images shown are from injections performed with a single microneedle of 700 µm length (Single), a row of microneedles of 600 µm length (Row), or a single microneedle of 400 µm length (Short). The red dashed line indicates the epidermal/dermal junction (epidermis above and dermis below the line). The red asterisk indicates the insertion point, the yellow asterisks mark the clusters of injected cells, and the yellow arrows point at the cells injected in the basal layer. (B) Confocal microscopy images of cryosections of excised human skin injected with labelled ECS and incubated with anti melan-A and anti involucrin antibodies show that the injected cells (blue nuclei) maintain their melanocytic (green cytoplasm, green arrow) or keratinocytic (red cytoplasm, red arrow) phenotype after delivery. Scale bars = 100 µm.

327x150mm (150 x 150 DPI)